

Synergistic Effects of Expandable Graphite and Ammonium Polyphosphate with a New Carbon Source Derived from Biomass in Flame Retardant ABS

Yan Zhang,¹ Xiaoling Chen,^{1,2} Zhengping Fang^{1,2}

¹Laboratory of Polymer Materials and Engineering, Ningbo Institute of Technology, Zhejiang University, Ningbo 315100, China

²MOE Key Laboratory of Macromolecular Synthesis and Functionalization, Department of Polymer Science and Engineering, Zhejiang University, Hangzhou 310027, China

Correspondence to: Z. Fang (E-mail: zpfang@zju.edu.cn)

ABSTRACT: A novel flame retardant system, ammonium polyphosphate (APP), and expandable graphite (EG) with a new carbon source, poly(diphenolic phenyl phosphate) (poly(DPA-PDCP)), derived from biomass has been proven to be effective in preventing melting drip and improving flame retardancy of acrylonitrile–butadiene–styrene copolymer (ABS) in this study, which was manifested by limiting oxygen index (LOI) and vertical flammability (UL-94) tests. The optimal synergy was exhibited at a loading of 30 wt % of three flame retardants in a proper ratio (APP/poly(DPA-PDCP)/EG = 12/3/15). Thermogravimetric analysis result indicated the char residue and the thermal stability could be enhanced because of the synergistic effect of APP/poly(DPA-PDCP)/EG, which is elaborated by a hypothesis of flame retardancy mechanism of the three components. The morphologies of cross-section and char residue by SEM were also described. The dynamic mechanical analysis implied that APP/poly(DPA-PDCP)/EG together can enhance the dynamic mechanical property of ABS. © 2012 Wiley Periodicals, Inc. *J. Appl. Polym. Sci.* 000: 000–000, 2012

KEYWORDS: flame retardance; thermogravimetric analysis; thermal properties; blends

Received 6 April 2012; accepted 23 July 2012; published online

DOI: 10.1002/app.38382

INTRODUCTION

Acrylonitrile–butadiene–styrene copolymer (ABS) was widely used in many applications due to its good mechanical and physical properties such as processability, toughness, impact resistance, and excellent appearance.^{1,2} However, it has deemed as one of the most difficult polymers to flame retard because of its extreme flammability and melt dripping, which has attracted considerable interest during the last decades.^{3,4}

Although traditional halogen-contained compounds improved the flame retardancy of ABS significantly, there is an increasing restriction about their use because they produce a large amount of smoke, toxicity and corrosion gases during combustion.^{5,6} Because intumescent flame retardant (IFR) systems are halogen-free and are believed to be environmentally friendly, they have attracted great attention in recent years.^{7–11}

One characteristic of IFR systems is their formation of insulative, foamed, carbonaceous chars.¹² The blown cellular char produced from the synergistic interaction among acid source, blowing agent and carbonic source in the intumescent flame retardant system to prevent the underlying material from heat

and mass transfer. The carbonic sources are usually polyols such as pentaerythritol, mannitol, and sorbitol.^{13,14} However, these carbonization agents have drawbacks such as moisture absorption, exudation, and incompatibility with the polymeric matrix. So, a lot of work has recently been done on applications of different kinds of carbonization agents.^{4,15–19}

In our previous study, diphenolic acid (DPA), which is produced on large scale from phenol and levulinic acid, a potential platform chemical from biomass,^{20–22} was reacted with phenyl dichlorophosphate (PDCP) by interfacial polycondensation to synthesize a novel phosphorus-contained flame retardant, poly(diphenolic phenyl phosphate) (poly(DPA-PDCP)), which is shown in Figure 1. Thermogravimetric analysis (TGA) denotes that the residue of poly(DPA-PDCP) at 600°C is 46%, indicating its good char-forming ability.²³ The solubility tests also exhibited its good solvent-resistant (including water) property. However, since there is an active carboxyl in poly(DPA-PDCP), the formation of water and carbon dioxide by carboxyls begin at the temperature of 200°C, which is earlier than that of the stable char layer formation. Therefore, the flame retardant ABS with poly(DPA-PDCP) alone or combined with APP as flame

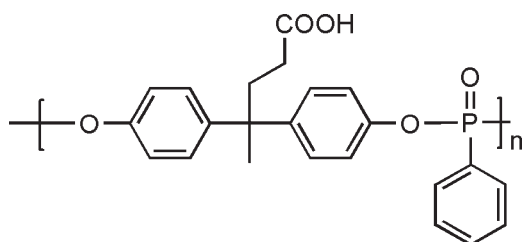


Figure 1. Structure of poly(DPA-PDCP).

retardant failed to achieve UL-94 V-0 rating. It seems that there are big spaces to optimize this novel flame retardant system. On the other hand, from the viewpoint of environmental protection, the study of bio-based flame retardant system favors sustainable development of flame retardant industries because of the increasingly serious energy resource crisis.

In this work, expandable graphite (EG), was selected as a synergistic additive of the flame retardant ABS system with poly(DPA-PDCP) and APP, which has been deemed as a blowing agent and a smoke suppressor in a growing number of fire-retardant applications.^{24–26} When exposed to heat, EG can expand and generate a voluminous insulative layer to protect the polymeric matrix.^{27,28} According to this characteristic of EG, we expect that the insulative layer built by EG can act as gas blocker to hamper the incombustible gas produced by poly(DPA-PDCP) or/and APP during combustion and a novel improved flame retardant system would be obtained. Therefore, the aim of this work was to study the effects of APP, poly(DPA-PDCP), and EG, whether or not they can synergistically improve the flame retardant properties of ABS. The flammability of the materials was evaluated via UL-94 tests and LOI tests. Thermal degradation behavior and char structure were investigated using thermo gravimetric analysis (TGA) and scanning electron microscope (SEM). The dynamic mechanical analysis (DMA) was applied to characterize mechanical property of the flame retardant ABS.

EXPERIMENTAL

Raw Materials

Poly(DPA-PDCP) was synthesized and purified as previously reported.²³ Ammonium polyphosphate (APP) ($n = 1500$) was supplied by Hangzhou JLS Flame Retardants Chemical, China. ABS (HI-121H) was purchased from LG Petrochemical Company, Korea. Expandable graphite (EG) with practical size of $180 \mu\text{m}$ and expansion volume of 150 is supplied by Baoding Action Carbon, China.

Preparation of Flame-Retardant ABS

All the samples (ABS/Poly(DPA-PDCP)/APP/EG) were melt-mixed at 190°C using ThermoHaake rheomixer with a rotation speed of 60 rpm, and the mixing time was 8 min. After mixing, the samples were transferred to a mold and hot-pressed under 15 MPa for 5 min at 190°C , and then pressed under 15 MPa for another 5 min at room temperature. The mold size and thickness were dependent on the testing method used in the study. According to our previous study, the optimized formulation of APP and poly(DPA-PDCP) in flame retardant is as

followed: the ratio of APP and poly(DPA-PDCP) is 4:1 and the total loading of the flame retardant is 30 phr. So, considering the practice application, we use the total amount 30 phr of FR additives including APP, poly(DPA-PDCP) and EG and the ratio of APP/poly(DPA-PDCP) about 4:1 as a reference. The formulations of ABS samples are showed in Table I.

Measurements

Thermogravimetric Analysis (TGA). Thermogravimetric analysis (TGA) was done in a TG209F1 thermal analyzer (Netzsch, Germany) at a scanning rate of $20^\circ\text{C min}^{-1}$ under air, from 30 to 650°C .

Limiting Oxygen Index (LOI). The LOI measurement was carried out according to ASTM D2863-00. The apparatus used was an HC-2 instrument (Jiangning Analysis Instrument, China). The size of sample was $130 \times 6 \times 3 \text{ mm}^3$.

UL-94 Vertical Test. The vertical test was performed according to the fifth edition (2010) of UL 94-1996 standard with a CTF-2 vertical burning instrument (Jiangning Analysis Instrument, China). The specimens used were of $125 \times 12.7 \times 3.2 \text{ mm}^3$.

Scanning Electron Microscopy (SEM). The fractured surfaces of original samples and char residues after LOI test were first sputter-coated with a conductive layer, and then its surface morphology was observed by an S-4800 field emission scanning electron microscope (Hitachi, Japan) with a 5 kV accelerated voltage to study the dispersion of EG.

Dynamic Mechanical Analysis (DMA). Dynamic mechanical analysis was performed using a DMA-242C dynamic mechanical analyzer (Netzsch, Germany). The tests were carried out in single-point bending mode at a vibration frequency of 1 Hz in a temperature range from 20 to 150°C at a heating rate of 5°C min^{-1} under nitrogen. The sizes of samples were $35 \times 10 \times 1.2 \text{ mm}^3$.

RESULTS AND DISCUSSION

Morphology and Structure

The dispersion state of EG is one of the key factors affecting the fire-retardant properties of polymers.²⁹ To determine the dispersion state of EG in ABS, SEM analysis was carried out at the fractured surfaces of samples from ABS-III to ABS-VI and the

Table I. Formulation for Flame Retarded ABS/Poly(DPA-PDCP)/APP/EG Composites

Sample ID	ABS (wt %)	APP (wt %)	Poly(DPA-PDCP) (wt %)	EG (wt %)
ABS-I	100	0	0	0
ABS-II	70	24	6	0
ABS-III	70	20	5	5
ABS-IV	70	16	4	10
ABS-V	70	12	3	15
ABS-VI	70	0	0	30
ABS-VII	70	15	0	15
ABS-VIII	70	0	15	15

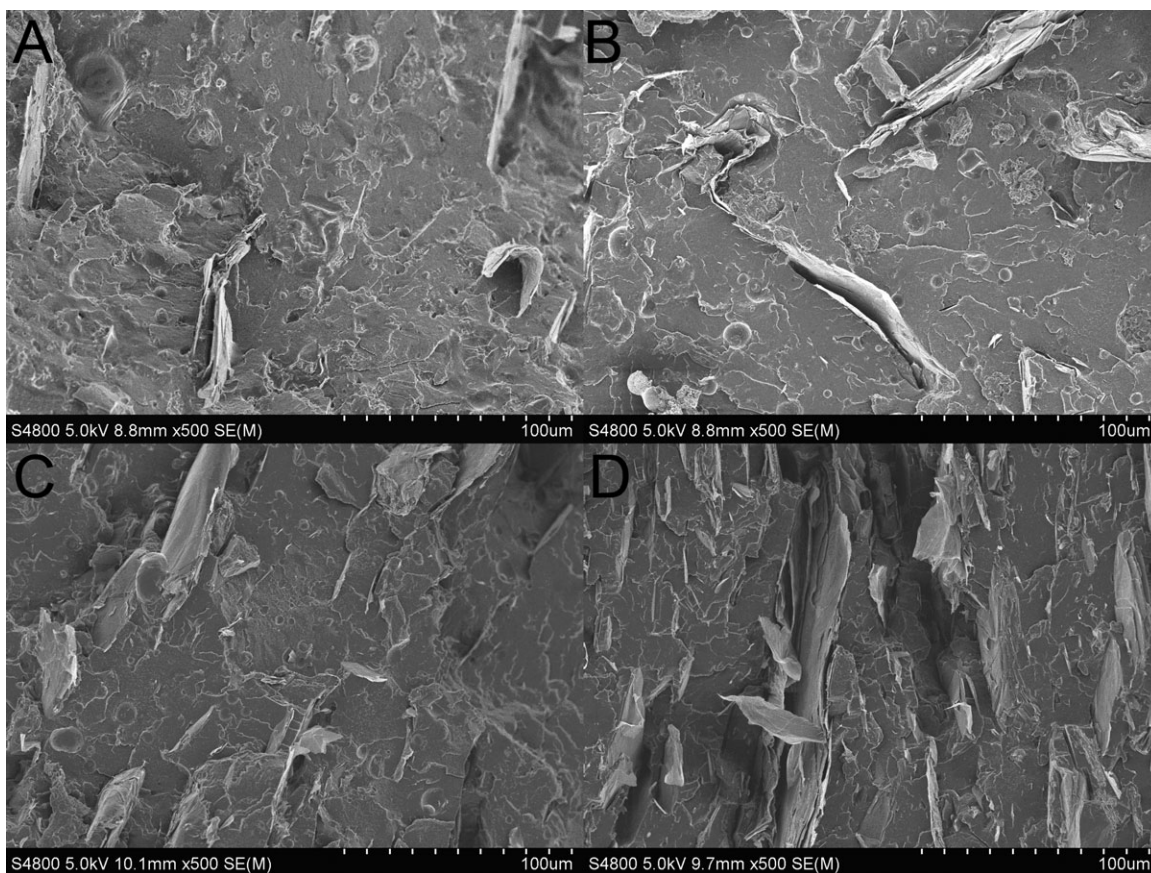


Figure 2. Morphology of ABS/APP/Poly(DPA-PDCP)/EG composites (A) ABS-III, (B) ABS-IV, (C) ABS-V, (D) ABS-VI.

results are shown in Figure 2. As Figure 2 shows, flake-like EG particles dispersed in the matrix with the size of 80–150 μm . Compared with the initial size, the flake structures of EG became smaller because shearing of rotors resulted in the breakage of EG flakes during the mixing process. With the increase of EG, overlap between EG layers and agglomerates appeared in Figure 2(C, D). Because the addition of EG results in great viscosity increase, especially for high EG content, the increased viscosity makes it more difficult to disperse the EG particles.²⁷ Although extending mixing time and increasing rotation speed can improve the dispersion state of EG in matrix, the modification of the EG size will result in poor fire retardant properties for matrix, which is ascribed to its insufficient expansion volume to cover the burning surface.²⁹ So the processing to prepare ABS/EG composites should be controlled with suitable mixing time and rotation speed.

Thermal Behavior of Flame Retardant ABS

Figure 3 and Table II exhibits the thermogravimetric (TG) behavior and data of pure ABS and ABS composites with APP/poly(DPA-PDCP)/EG as flame retardants under air. All the samples showed two-stage degradation. As for pure ABS, the first stage is observed in the temperature range of 300–500°C due to the degradation of styrene-acrylonitrile copolymer (SAN) phase.^{30–32} The residue formed at the first stage continued to degrade at the second stage from 500 to 600°C, which leads to 0 wt % residues at the end of the degradation.

With the loading of 24 phr APP and 6 phr poly(DPA-PDCP) (ABS-II), the onset decomposition temperature (T_{onset}) of ABS-II composite is lower than that of pure ABS by 52°C, however, the char residue increases to 20% and the peak temperatures of two-stage degradation of flame retardant ABS increased by 9 and 56°C, respectively, which indicates that APP and poly(DPA-PDCP) enhances the thermal stability and char-forming ability of ABS. After the addition of EG with different contents, the residue for the composites are higher than that without EG at the high-temperature range from 450 to 600°C. This is because a more stable and thick expanded char is formed between the fire and the matrix to prohibit further decomposition. The T_{onset} of samples from ABS-III to ABS-V decreased by 14–40°C, which is assigned to the scission of the phosphate ester bonds of poly(DPA-PDCP)/APP and the release of blowing gases originated by the graphite. However, the curves of derivatives versus temperature were observed shifting to higher temperature of 392–409°C and the maximal weight loss rate decreased to 24.2% per min in ABS-V even lower than that of ABS-VI with EG alone, suggesting that the rate of degradation was slowed down by the cooperation of APP, poly(DPA-PDCP) and EG. All the above results indicate that the addition of APP/poly(DPA-PDCP)/EG decreases the thermal stability of ABS at the initial decomposition stage and increases the thermal stability at the higher temperature because of complementary mechanisms of the three component in ABS. The hypothesis of flame retardancy mechanism is shown in Figure 4.

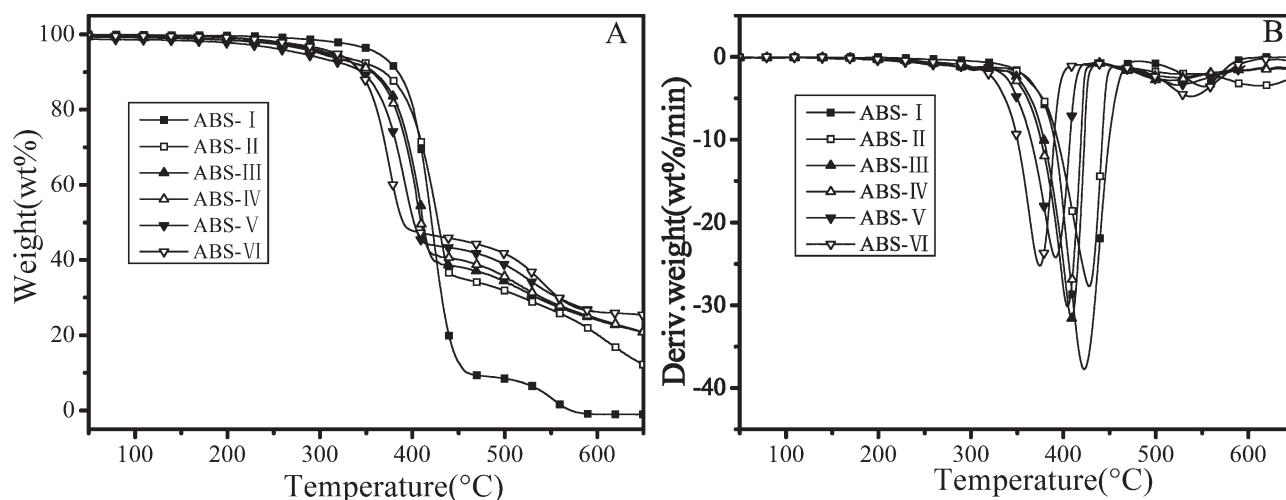


Figure 3. (A) TG and (B) DTG curves of ABS and flame retarded ABS formulations in air.

As Figure 4 shows, anhydride product formed by the condensation of carboxyl groups of poly(DPA-PDCP) will carry out further decarboxylation to result in the crosslink of itself with increasing temperature, which tends to form a carbonaceous char. Such crosslink is the primary reason for its good char-forming property. At the same time, this anhydride product can also have esterification with the oxidation products of SAN chain in ABS to bring out another crosslink between poly(DPA-PDCP) and matrix and result in the improved thermal stability of ABS, which is evident in the increase of T_{\max} of ABS-II. The existence of APP also contributed to this improvement. Seen from Figure 4, phosphoric and polyphosphoric acids produced by APP and the oxidation products of SAN chain have the reaction of esterification to form more stable structure with phosphorus element,^{33,34} which also accelerate the carbonization to yield more char residue.

Because EG could promote the creation of carbonaceous barrier inhibiting the release of the degraded products,³⁵ the vapor H_2O , CO_2 , and NH_3 formed by poly(DPA-PDCP) and APP can be caught by EG flakes, which accelerate the expansion of EG to obtain an intumescent graphite system. In this flame retardant system, EG not only acts as an insulation barrier to hamper the release of incombustible gas, but also has a redox process (shown in Figure 4) between residual H_2SO_4 from the EG production process and the graphite that originates blowing gases,

which causes an increase of the volume of the materials by about 150 times on heating above $200^\circ C$. The expanded graphite flakes will inhibit the fire and heat from attacking the polymer matrix. With the blend of APP/poly(DPA-PDCP)/EG in a proper ratio, the higher T_{\max} and residue char of flame retardant ABS was obtained in sample ABS-V.

Comparing ABS-V with ABS-VI, the differences of the char residue at $600^\circ C$ and maximum weight loss rate are not obvious except the increased T_{\max} of the first degradation of ABS-V. This unobvious apparent synergistic effect among APP/poly(DPA-PDCP)/EG is due to the low quantity (about 5–7 mg) of the samples for the TGA measurements since physical effects of flame retardancy will not be observed in small milligram samples where weight loss is being measured. The better flame retardancy of sample ABS-V will be clearly showed in the results of the following LOI and UL-94 tests.

The above thermogravimetric analysis under air can be deemed as the combustion of the sample under designed temperatures. However, as is known to all, once a sample ignites, all oxygen is consumed at the flame front, meaning in fires that TGA under nitrogen is a very important test condition for determining how a material will behave. Therefore, the thermogravimetric behavior and data of pure ABS and ABS composites with APP/poly(DPA-PDCP)/EG under N_2 was also investigated and the data were collected in Figure 5 and Table III. Compared with TG

Table II. Detailed Data Obtained from TG and DTG of ABS and Flame Retarded ABS in Air

Sample ID	T_{onset} ($^\circ C$)	T_{\max} ($^\circ C$)		Residue (wt %)			D_{pk} (%/min)
		Stage 1	Stage 2	T_{450}	T_{500}	T_{600}	
ABS-I	362	423	553	12	9	0	37.8
ABS-II	310	432	609	36	31	20	27.8
ABS-III	304	409	525	38	34	24	31.5
ABS-IV	300	405	525	40	37	25	30.0
ABS-V	278	392	523	42	39	26	24.2
ABS-VI	318	375	538	45	41	26	25.3

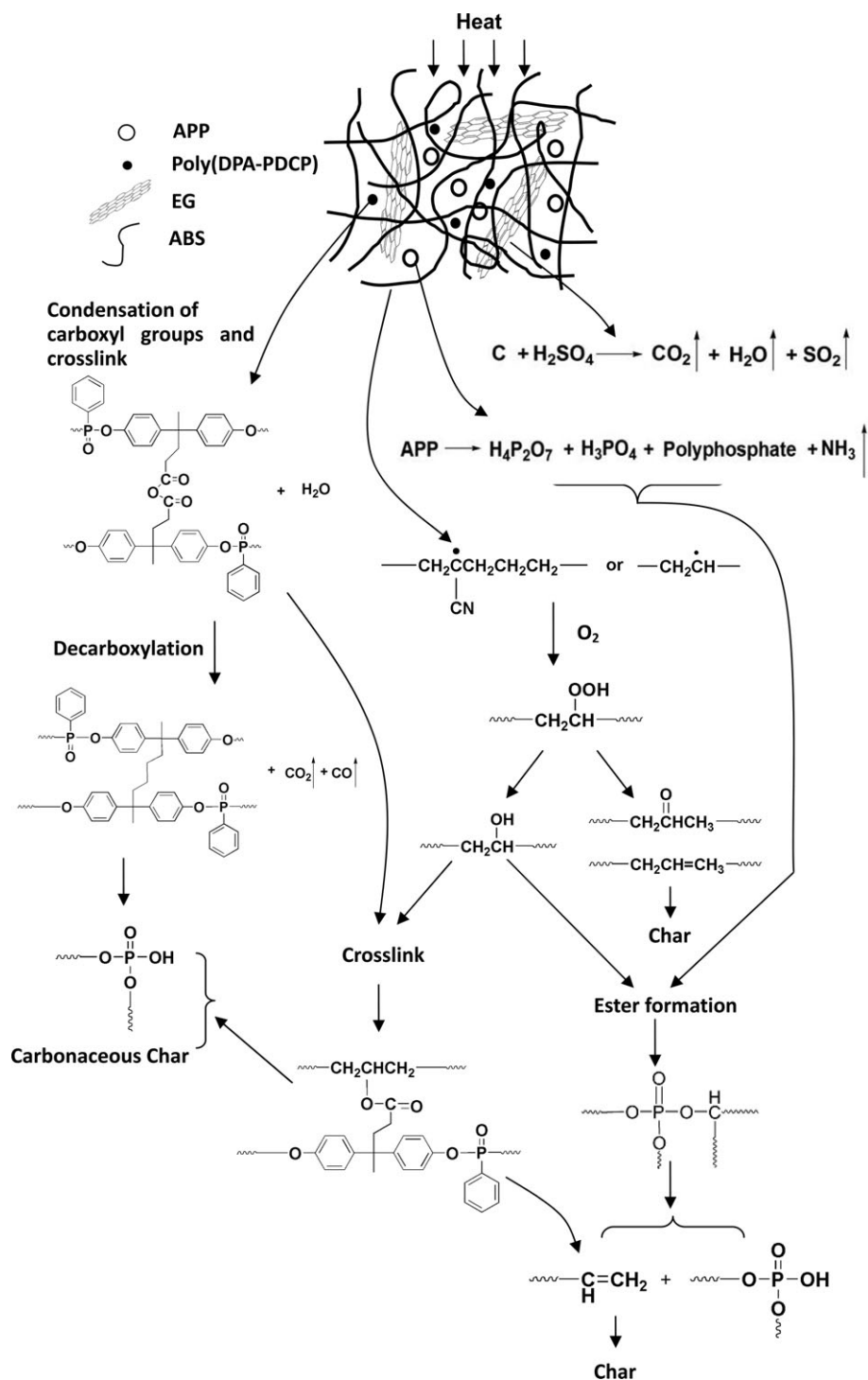


Figure 4. Mechanism of flame retardant ABS with APP/poly(DPA-PDCP)/EG.

curves in air, all samples essentially degrade in a single step except for flame retardant ABS samples with APP and poly (DPA-PDCP). The first stage with the T_{max} about 288–293°C can be ascribed to the early decomposition of phosphate ester bonds of APP and poly(DPA-PDCP).

It can be seen from the results that the pure ABS leaves negligible char above 500°C. With the increase of the content of EG, the amount of char residue increased from 20 to 29% and the

maximal weight loss rate decreased to 26.5% per min. However, it is found that the T_{max} s at the second stages decreased from 432 to 424°C obviously. This is because that although the EG can act mainly in the condensed phase by forming an intumescent layer of worm-like expanded graphite,³⁶ brittle EG layers would be formed with the decreased amount of APP,^{7,37} which can't generate enough and stabler char from resin. It is interesting that the existence of poly(DPA-PDCP) didn't show as

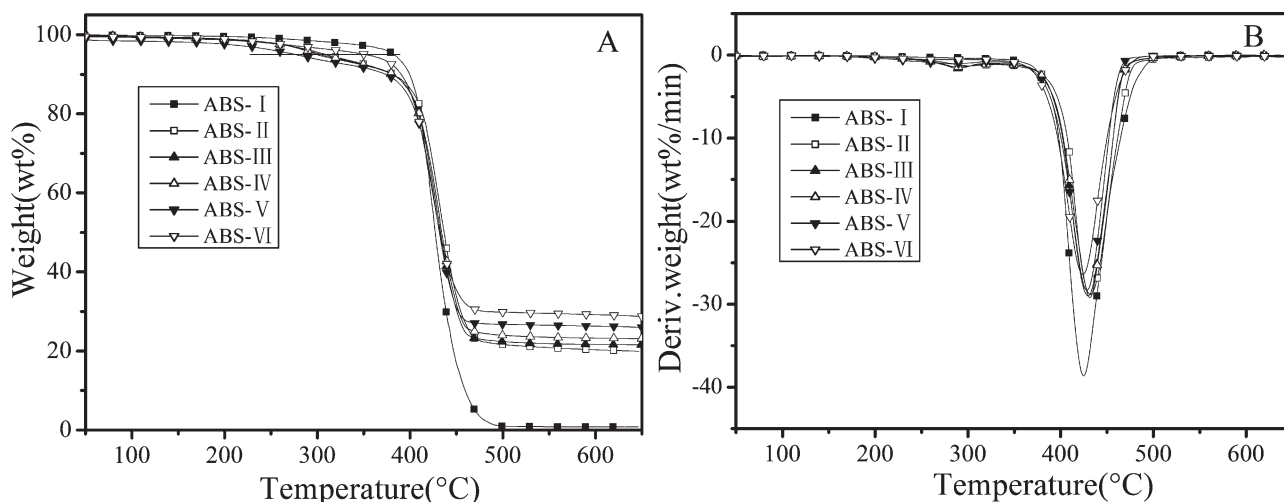


Figure 5. (A) TGA and (B) DTG curves of ABS and flame retarded ABS formulations in N_2 .

obvious contribution to the improvement of the thermal stability of ABS as that in air, which is due to the N_2 atmosphere in TGA. As shown in Figure 4, this anhydride product formed by poly(DPA-PDCP) can have esterification with the oxidation products of SAN chain in ABS to bring out the crosslink between poly(DPA-PDCP) and ABS, and result in the improved thermal stability of ABS. While, the oxidation reaction of SAN chain in ABS is hardly to carry out without oxygen and the crosslink between poly(DPA-PDCP) and ABS can't be generated, either. That is to say, poly(DPA-PDCP) can form the crosslink of itself and there is little obvious interaction between poly(-DPA-PDCP) and polymers. Therefore, the synergistic effect among APP/poly(DPA-PDCP)/EG in N_2 is not as obvious as that in air.

Flammability Properties of Flame Retardant ABS

The flammability properties of flame retardant ABS were analyzed by the limiting oxygen index (LOI) and UL-94 vertical burning tests and the data are listed in Table IV. As for pure ABS, LOI value of 19.5% indicated its flammable nature. As for samples ABS-II ~ABS-V, with the increase of EG content, the LOI values increase from 25.2 to 32.6%. The vertical burning test also shows the same trend. At the low loading of EG, flame impingement of ABS-II and ABS-III are longer than 30 s and burned with flaming dripping, thus they cannot be classified by the vertical burning test. After combining APP/poly(DPA-

PDCP) with more EG in ABS, dripping phenomenon and the rating of UL-94 test were both remarkably improved (V-2 rating for ABS-IV and V-0 rating for ABS-V), which is also evident in the photographs of the samples of ABS-III, ABS-IV and ABS-V after UL94 vertical tests in Figure 6. It can be seen that the melted-form residues of ABS were improved with the change of the ratio of APP/poly(DPA-PDCP)/EG. The pointed shape formed at the ignition side due to flame dripping was gradually changed to an obvious swollen char residue. However, when the flame retardant is EG alone, the sample ABS-VI failed in UL94 test because of the serious molten drop during combustion. To confirm the influence of poly(DPA-PDCP), samples ABS-VII (APP/EG=1/1, without poly(DPA-PDCP)) and ABS-VIII (poly(-DPA-PDCP)/EG=1/1, without APP) were also prepared. Compared with ABS-V, although the sample ABS-VII passed UL94 V-0 rating, the LOI values decreased to 24.2%; the sample ABS-VIII failed in UL94 test and burned to the clamp during combustion.

Seen from the data of Table IV, it can be concluded that the interaction of the three flame retardants in a proper ratio can result in a synergistic effect with better flame retardancy. According to the mechanism shown in Figure 4, a crosslink structure can be obtained through the reaction between anhydride formed by poly(DPA-PDCP) and the oxidation products of SAN chain in ABS, which will increase the melt viscosity of

Table III. Detailed Data Obtained from TG and DTG of ABS and Flame Retarded ABS in N_2

Sample ID	T_{onset} (°C)	T_{max} (°C)		Residue (wt %)			D_{pk} (%/min)
		Stage 1	Stage 2	T_{450}	T_{500}	T_{600}	
ABS-I	388	-	424	18	1	1	38.6
ABS-II	309	293	432	33	21	20	28.8
ABS-III	300	288	430	32	22	22	29.2
ABS-IV	304	288	432	32	23	23	29.0
ABS-V	278	290	428	31	27	26	28.3
ABS-VI	352	-	424	35	29	29	26.5

Table IV. Limiting Oxygen Index (LOI) and UL94 Rating of ABS and Flame Retarded ABS

Sample ID	Limiting oxygen index (%)	UL-94 rating	Melt dripping
ABS-I	19.5	-	Y
ABS-II	25.2	Failed	Y
ABS-III	25.2	Failed	Y
ABS-IV	27.3	V-2	Y
ABS-V	32.6	V-0	N
ABS-VI	30.5	Failed	Y
ABS-VII	24.2	V-0	N
ABS-VIII	17.6	Failed	Y

ABS to restrict the formation of melting drop during combustion. As the mentioned ahead, the addition of EG in ABS also results in the increase of viscosity. Therefore, melting drop can be greatly improved by the cooperation of poly(DPA-PDCP) and EG. On the other hand, APP plays an important role to induce more char from resin. When the loading of EG is less, char layer and viscosity increase formed by EG will be insufficient, which results in lower flame retardant efficiency and serious melt dripping. Yet when the addition of APP isn't sufficient, the brittle EG layers would be formed without the induction of char from resin by APP,^{7,37} which affect the fire property especially UL-94. When the EG and APP is used without poly(DPA-

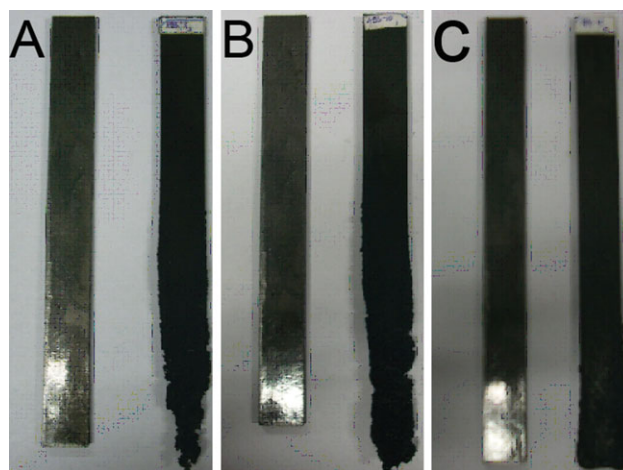


Figure 6. Digital photos of flame retarded ABS after UL-94 tests: (A) ABS-III, (B) ABS-IV, (C) ABS-V.

PDCP), the crosslink formed between poly(DPA-PDCP) and polymer chains can't be generated, which affect the formation of compact char with sufficient strength and lower the value of limiting oxygen index. Therefore, poly(DPA-PDCP) plays an important role in this flame retardant system, which influences the flame retardancy of ABS and should be cooperated with APP and EG in a proper ratio (ABS-V: APP/poly(DPA-PDCP)/EG = 12/3/15) to achieve a better flame retardancy.

Figure 7 is the SEM micrographs for char residue [Figure 7(A, B)] and the inside after removing the upper layer [Figure 7(C,

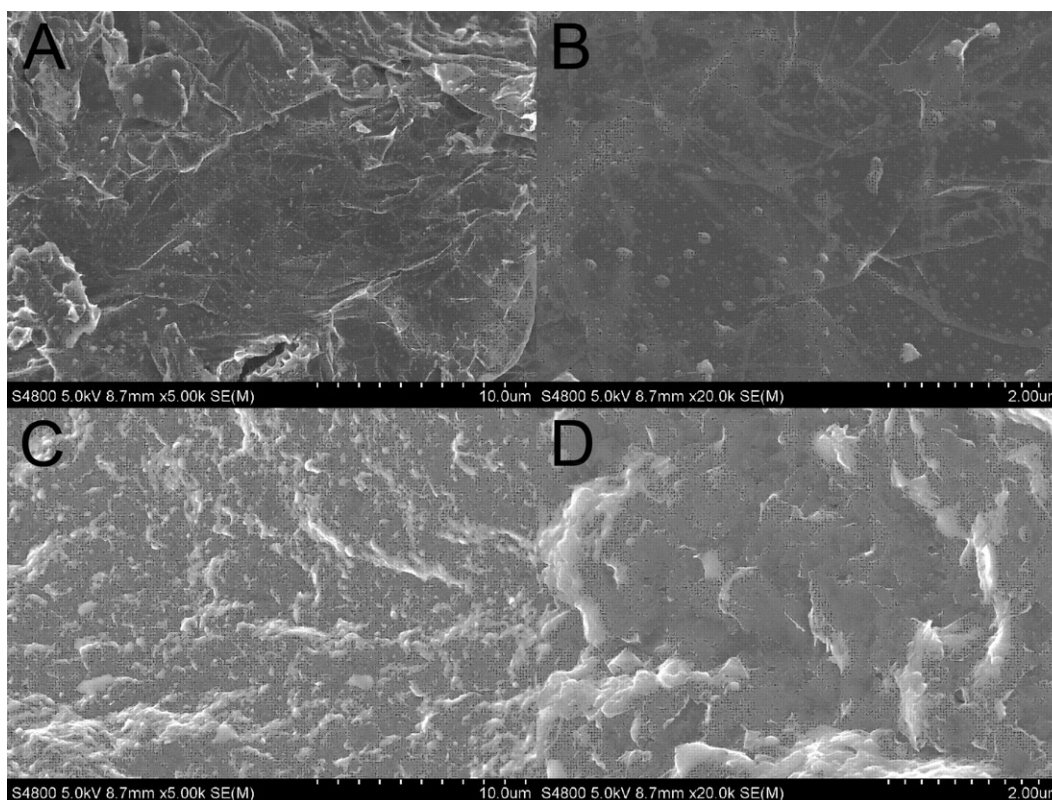


Figure 7. SEM micrographs of outer surface (A, B) and inner surface (C, D) of the residues of ABS-V after LOI tests.

D)] of sample ABS-V after LOI test. As seen from Figure 7(A, B), a dense and continuous char layer with small particles were formed during combustion. According to the aforementioned, the combination of the char from ABS resin induced by APP and carbonaceous char layer created by EG can contribute to such continuous char layer without holes or gaps, which lead to a good flame retarded performance. The small particles can be ascribed to the crosslink products formed by the esterification between SAN chains and poly(DPA-PDCP) and decomposition of poly(DPA-PDCP) itself, which stick in the char layer to form more compact char with sufficient strength to protect the matrix from fire and heat. Figure 7(C, D) is photos for the inside morphology after removing the upper layer, showing obvious unburned polymeric materials. It was indicated that the char formed by the flame retardants combined by APP, poly(DPA-PDCP) and EG did act as an effective barrier to protect the underlying substance from further burning.

Dynamic Mechanical Properties

The dynamic mechanical properties including storage modulus (E') and the damping factor ($\tan \delta$) of ABS and its blends with flame retardants between 20 and 150°C were shown in Figures 8 and 9, respectively. As seen from Figure 8, E' of the pure ABS and ABS blends has a slow drop below the glass-transition temperature (T_g) and decreases sharply through the glass-transition process. The E' of the ABS blends is higher than that of the pure ABS within the temperature range of testing except for ABS-II, which is lower than the pure ABS when the temperature is over 105°C because of the plasticization effect of APP/poly(DPA-PDCP). The E' values of ABS-III, ABS-IV and ABS-V is between that of the pure ABS and ABS-VI below 125°C, which indicates good interfacial adhesion between the flame retardant filler and the matrix system. Figure 8 also shows that the values of E' are close for ABS-V and ABS-VI below 40°C and for ABS-III and ABS-IV below 85°C, respectively. The values of E' of ABS-V and ABS-VI are higher than that of ABS-III and ABS-IV, which maybe ascribe to the different interfacial adhesion of APP/poly(DPA-PDCP) and EG with ABS. The above results imply that the addition of APP/poly(DPA-PDCP)/EG to-

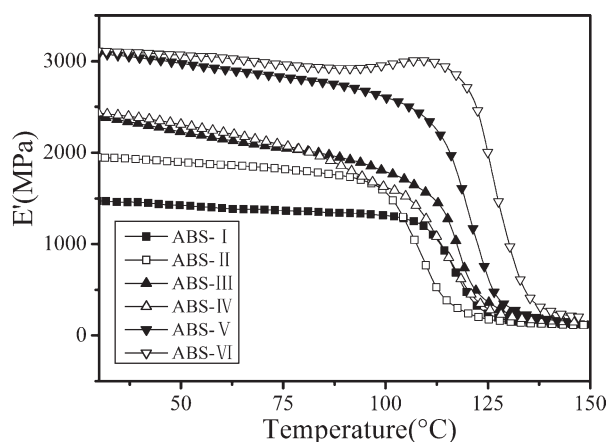


Figure 8. The storage modulus (E') for flame retarded ABS formulations as a function of the temperature.

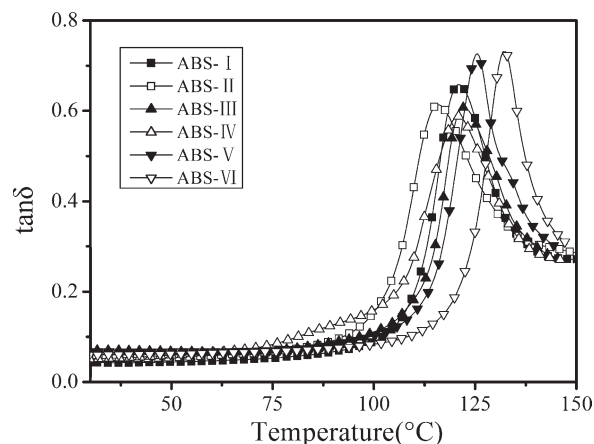


Figure 9. Loss tangents ($\tan \delta$) for flame retarded ABS formulations as a function of the temperature.

gether can enhance the dynamic mechanical property of ABS at a certain extent.

To determine application temperature of the flame retardant ABS, T_g was measured by DMA at the maximum of $\tan \delta$, which is shown in Figure 9. Because of the plasticization effect of APP/poly(DPA-PDCP), the value of $\tan \delta$ of ABS-II is lower than that of pure ABS and other ABS blends. After the addition of EG, the motion of polymer chain was hampered and the T_g was increased with the content of EG and the value of $\tan \delta$ are always higher than that of pure ABS.

CONCLUSIONS

The IFR system containing APP, poly(DPA-PDCP) and EG improved the flame retardancy of ABS. LOI values above 32.6% and the UL-94 test V-0 level could be obtained with a decreased dripping tendency, since crosslink structure induced by poly(DPA-PDCP) and the barrier effect brought by EG could increase the melt viscosity of ABS to restrict the melt dripping during combustion. TG results indicated that the addition of APP/poly(DPA-PDCP)/EG decreased the thermal stability of ABS at the initial decomposition stage and increased the thermal stability at the higher temperature. These results are consistent with the analysis of morphologies by SEM. The optimal synergism was found for ABS/APP/poly(DPA-PDCP)/EG systems when the three components of the flame retardant system was in a proper ratio (ABS-V: APP/poly(DPA-PDCP)/EG = 12/3/15). The hypothesis of flame retardancy mechanism was brought out to elaborate the synergistic effect of the three components in ABS. The dynamic mechanical analysis implied that the addition of APP/poly(DPA-PDCP)/EG together can enhance the dynamic mechanical property of ABS with the increased E' and T_g . As the scarcity of nonrenewable petroleum resource becomes increasingly serious problem, using chemicals derived from biomass to obtain flame retardant will be a potential approach for sustainable development of IFRs and need to be studied further.

ACKNOWLEDGMENTS

Financial supports from the National Basic Research Program of China (No.2010CB631105), technological innovation team work

project of Zhejiang province (No. 2009R50004), and the Natural Science Foundation of Zhejiang Province (No. Q12E030019) are acknowledged.

REFERENCES

- Choi, Y. S.; Xu, M. Z.; Chung, I. J. *Polymer* **2005**, *46*, 531.
- Ma, H. Y.; Tong, L. F.; Xu, Z. B.; Fang, Z. P.; Jin, Y. M.; Lu, F. Z. *Polym. Degrad. Stabil.* **2007**, *92*, 720.
- Hoang, D. Q.; Kim, J.; Jang, B. N. *Polym. Degrad. Stabil.* **2008**, *93*, 2042.
- Jun, W.; Yi, J. S. Cai, X. F. *J. Appl. Polym. Sci.* **2011**, *120*, 968.
- Lu, S. Y.; Hamerton, I. *Prog. Polym. Sci.* **2002**, *27*, 1661.
- Sen, A. K.; Mukherjee, B.; Bhattacharya, A. S.; Sanghi, L. K.; De, P. P.; Bhowmic, K. *J. Appl. Polym. Sci.* **1991**, *43*, 1673.
- Zhu, H. F.; Zhu, Q. L.; Li, J.; Tao, K.; Xue, L. X. Yan, Q. G. *Polym. Degrad. Stabil.* **2011**, *96*, 183.
- Camino, G.; Costa, L.; Trossarelli, L. *Polym. Degrad. Stabil.* **1985**, *12*, 213.
- Camino, G.; Martinasso, G.; Costa, L. *Polym. Degrad. Stabil.* **1990**, *27*, 285.
- Smith, R.; Georlette, P.; Finberg, I.; Reznick, G. *Polym. Degrad. Stabil.* **1996**, *54*, 167.
- Bourbigot, S.; Le Bras, M. *Fire. Mater.* **1996**, *20*, 145.
- Gao, M.; Wu, W.; Yan, Y. *J. Therm. Anal. Calorim.* **2009**, *95*, 605.
- Le Bras, M.; Bourbigot, S.; Delporte, C.; Siat, C.; Tallec, Y. L. *Fire. Mater.* **1996**, *20*, 191.
- Le Bras, M.; Bourbigot, S.; Tallec, Y. L.; Laureyns, J. *Polym. Degrad. Stabil.* **1997**, *56*, 11.
- Ke, C. H.; Li, J.; Fang, K. Y.; Zhun, Q. L.; Yan, Q.; Wang, Y. Z. *Polym. Degrad. Stabil.* **2010**, *95*, 763.
- Dai, J. F.; Li, B. *J. Appl. Polym. Sci.* **2010**, *116*, 2157.
- Liu, Y. Z.; Feng, Z. Q.; Wang, Q. *Polym. Compos.* **2009**, *30*, 221.
- Lu, C. X.; Chen, T.; Cai, X. F. *J. Macromol. Sci. B.* **2009**, *48*, 651.
- Zhang, Y. X.; Liu, Y.; Wang, Q. *J. Appl. Polym. Sci.* **2010**, *116*, 45.
- Zhang, P.; Wu, L. B.; Bu, Z. Y.; Li, B. G. *J. Appl. Polym. Sci.* **2008**, *108*, 3586.
- Zhang, P.; Wu, L. B.; Bu, Z. Y.; Li, B. G. *Polym. Degrad. Stabil.* **2009**, *94*, 1261.
- Bozell, J. J.; Moens, L.; Elliott, D. C.; Wang, Y.; Neuenschwander, G. G.; Fitzpatrick, S. W.; Bilski, R. J.; Jarnefeld, J. L. *Resour. Conserv. Recycl.* **2000**, *28*, 227.
- Zhang, Y.; Chen, X. L.; Fang, Z.P. *Adv. Mater. Res.* **2011**, *284*, 187.
- Modesti, M.; Lorenzetti, A.; Simioni, F.; Camino, G. *Polym. Degrad. Stabil.* **2002**, *77*, 195.
- Murariu, M.; Dechief, A. L.; Bonnaud, L.; Paint, Y.; Gallos, A.; Fontainel, G.; Bourbigot, S.; Dubois, P. *Polym. Degrad. Stabil.* **2010**, *95*, 889.
- Xie, R. C.; Qu, B. J. *Polym. Degrad. Stabil.* **2001**, *71*, 395.
- Meng, X. Y.; Ye, L.; Zhang, X. G.; Tang, P. M.; Tang, J. H.; Ji, X.; Li, Z. M. *J. Appl. Polym. Sci.* **2009**, *114*, 853.
- Duquesne, S.; Michel, L. B.; Bourbigot, S.; Delobel, R.; Vezin, H.; Camino, G.; Eling, B.; Lindsay, C.; Roels, T. *Fire. Mater.* **2003**, *27*, 103.
- Shi, L.; Li, Z. M.; Xie, B. H.; Wang, J. H.; Tian, C. R.; Yang, M. B. *Polym. Int.* **2006**, *55*, 862.
- Suzuki, M.; Wilkie, C. A. *Polym. Degrad. Stabil.* **1995**, *47*, 217.
- Grassie, N.; Bain, D. R. *J. Polym. Sci. Polym. Chem. Ed.* **1970**, *8*, 2653.
- Shapi, M. M.; Hesso, A. *J. Chromatogr.* **1991**, *562*, 681.
- Jang, J.; Kim, J.; Bae, J. Y. *Polym. Degrad. Stabil.* **2005**, *88*, 324.
- Bourbigot, S.; Le Bras, M.; Delobel, R.; Bréant, P.; Trémillon, J. M. *Carbon* **1995**, *33*, 283.
- Wei, P.; Li, H. X.; Jiang, P. K.; Yu, H. Y. *J. Fire. Sci.* **2004**, *22*, 367.
- Chuang, T. H.; Chern, C. K.; Guo, W. *J. Polym. Res.* **1997**, *4*, 153.
- Lu, Y. B.; Zhang, Y. J.; Xu, W. J. *J. Macromol. Sci. B.* **2011**, *50*, 1864.